Cite as: M. T. Kronschläger *et al.*, *Science* 10.1126/science.aah5715 (2016).

Gliogenic LTP spreads widely in nociceptive pathways

M. T. Kronschläger,* R. Drdla-Schutting,* M. Gassner, S. D. Honsek, H. L. Teuchmann, J. Sandkühler†

Department of Neurophysiology, Center for Brain Research, Medical University of Vienna, Spitalgasse 4, 1090-Vienna, Austria.

*These authors contributed equally to this work.

†Corresponding author. Email: juergen.sandkuehler@meduniwien.ac.at

Learning and memory formation involve long-term potentiation of synaptic strength (LTP). A fundamental feature of LTP induction in the brain is the need for coincident pre- and postsynaptic activity. This restricts LTP expression to activated synapses only (homosynaptic LTP) and leads to its input specificity. In the spinal cord, we discovered a fundamentally different form of LTP that is induced by glial cell activation and mediated by diffusible, extracellular messengers, including D-serine and tumor necrosis factor (TNF), and that travel long distances via the cerebrospinal fluid, thereby affecting susceptible synapses at remote sites. The properties of this gliogenic LTP resolve unexplained findings of memory traces in nociceptive pathways and may underlie forms of widespread pain hypersensitivity.

Activity-dependent, homosynaptic LTP (*1*) at synapses in nociceptive pathways contributes to pain amplification (hyperalgesia) at the site of an injury or inflammation (*2*–*5*). Homosynaptic LTP can, however, not account for pain amplification at areas surrounding (secondary hyperalgesia) or remote from (widespread hyperalgesia) an injury. It also fails to explain hyperalgesia that is induced independently of neuronal activity in primary afferents, e.g., by the application of, or the withdrawal from opioids (opioid-induced hyperalgesia) (*6*). Glial cells are believed to contribute to these forms of hyperalgesia and to LTP in nociceptive pathways (*7*–*10*). Induction of homosynaptic LTP can be accompanied by LTP in adjacent, inactive synapses converging onto the same neuron, especially early in development. The respective molecular signals for this heterosynaptic form of LTP are thought to be confined within the cytoplasm of the activated neuron spreading tens of micrometers only (*11*). We now tested the hypothesis that, in contrast to current beliefs, activation of glial cells is causative for the induction of LTP at spinal C-fiber synapses and that this gliogenic LTP constitutes a common denominator of homo- and heterosynaptic LTP in the spinal cord.

Our previous study revealed that selective activation of spinal microglia by fractalkine induces transient facilitation, but no LTP at C-fiber synapses (*12*). Here we recorded monosynaptic C-fiber-evoked excitatory postsynaptic currents (EPSCs) from lamina I neurons in rat lumbar spinal cord slices. To test if selective activation of spinal astrocytes is sufficient for the induction of synaptic plasticity in the absence of any other conditioning stimulus, we used UV-flash photolysis of caged IP_3 in astrocytic networks (fig. S1 and movie S1). This induced a robust long-term depression at C-fiber synapses (gliogenic LTD; to 69 ± 9%, $n = 7$, $P < 0.001$; fig. S1C) but no LTP. UV-flashes were without any effect on synaptic strength when applied in the absence of caged IP_3 (fig. S1D), or in presence of the glial cell toxin fluoroacetate (fig. S1E). To co-activate microglia and astrocytes, we next applied the purinergic $P2X_7$ receptor ($P2X_7R$) agonist BzATP. This never affected holding currents or membrane potentials in any of the spinal neurons tested (fig. S2) supporting the observation that, in the spinal dorsal horn, and unlike other P2X receptors (*13*), $P2X_7Rs$ are expressed exclusively on glial cells (*14*–*18*). ATP is finally hydrolyzed to adenosine. We therefore applied the adenosine 1 receptor antagonist DPCPX to block adenosine-mediated presynaptic inhibition (fig. S3). Combined activation of microglia and astrocytes by BzATP induced LTP in 13 out of 22 C-fiber inputs (to 156 ± 13%, $P < 0.001$; Fig. 1A). BzATP-induced LTP was abolished by the selective $P2X_7R$ antagonist A-438079 (Fig. 1B) and by fluoroacetate (Fig. 1C). This demonstrates that selective activation of $P2X_7R$ on spinal glial cells caused gliogenic LTP at synapses between C-fibers and lamina I neurons.

High frequency stimulation (HFS) of primary afferent C-fibers triggers the release of ATP from primary afferent neurons (*19*, *20*), activates glial cells (*21*, *22*), and induces LTP (*2*, *3*), leading to the intriguing hypothesis that HFS-induced LTP at spinal C-fiber synapses might be a variety of gliogenic LTP. If true, one would predict that HFS induces LTP not only at conditioned but also at unconditioned C-fiber synapses and that, in striking contrast to current beliefs, homo- and heterosynaptic LTP could be expressed independently of each other. To directly test these predictions we used transverse, lumbar spinal cord slices with long dorsal roots attached which were separated into halves. We recorded from 22 dorsal horn lamina I neurons that received independent monosynaptic C-fiber input from each dorsal root half. HFS applied to one dorsal root half induced LTP in the

conditioned pathway in 12 of these neurons ("homosynaptic LTP"; to 134 ± 9%, $P < 0.001$; Fig. 2Aa, red filled circles). Out of these 12 neurons, where homosynaptic LTP was induced, 6 also showed LTP at the unconditioned pathway ("heterosynaptic LTP"). In total, heterosynaptic LTP was induced in 11 out of 22 neurons (to 174 ± 19%, $P < 0.001$; Fig. 2Ba, blue filled circles) because importantly, in 5 of these neurons, heterosynaptic LTP was induced in the absence of homosynaptic LTP (to 161 ± 9%, $P < 0.005$; Fig. 2C), a finding that cannot be explained by current models of synaptic plasticity.

We tested if HFS-induced homo- and heterosynaptic LTP require activation of glial cells via $P2X_7R$. Blockade of glial $P2X_7R$ by A-438079 fully blocked LTP induction at the conditioned and at the unconditioned sites (Fig. 2Ab, Bb). This was also achieved by blocking glial cell metabolism with fluoroacetate [Fig. 2Ac, Bc and (*21*)]. Both, homo- and heterosynaptic LTP were abolished by blocking postsynaptic NMDARs (Fig. 2Ad, Bd). D-Serine is a co-agonist at NMDARs that is released from astrocytes (*23*). Here, preincubation of slices with the D-serine degrading enzyme D-amino acid oxidase (DAAO) abolished both, homo- and heterosynaptic LTP (Fig. 2Ae, Be). We then tested if D-serine alone is sufficient to enhance synaptic strength at C-fiber synapses. Bath application of D-serine facilitated synaptic strength at C-fiber synapses (to 120 ± 2% in 13 out of 32 cells, $P < 0.001$; fig. S4A). This amplification was abolished by blockade of NMDARs (in 12 out of 13 cells, $P = 0.094$; fig. S4B). Taken together our data demonstrate that the combined activation of microglia and astrocytes, either via $P2X_7R$ or by HFS was sufficient to induce gliogenic LTP. When gliogenic LTP is induced by conditioning HFS it may appear as homo- and / or heterosynaptic LTP that can be elicited independently of each other.

We next asked if gliogenic LTP also exists in vivo. HFS applied to the sciatic nerve induced LTP of spinal C-fiber-evoked field potentials in deeply anesthetized rats (to 211 ± 16% at 220 – 240 min, $n = 49$, $P < 0.001$; Fig. 3A). HFS-induced LTP was blocked by spinal application of either fluoroacetate (Fig. 3B) or DAAO (Fig. 3C) indicating that it required the activation of spinal glial cells and D-serine signaling. Application of fluoroacetate or DAAO after the induction of LTP had no effects on LTP maintenance (to 192 ± 23% and to 181 ± 30%, respectively, at 220 – 240 min, $n = 6$, $P = 0.433$ and $P = 0.546$; fig. S5) indicating that once LTP was induced glial cells were no longer required. Thus, the gliogenic nature refers to the induction but not to the maintenance phase of LTP.

We then tested if HFS leads to the release of diffusible mediators that spread over significant distances to trigger LTP. We induced LTP by HFS, collected the spinal superfusate from the respective lumbar segments and transferred it to the spinal cord dorsum of naïve animals. The maintenance of LTP in the donor animals was not affected by exchanging the superfusate (Fig. 3A). The superfusate induced, however, a robust LTP in the recipient animals (to 173 ± 32% of control at 160 – 180 min, $n = 10$, $P = 0.009$; Fig. 4A) demonstrating that LTP could be transferred between individuals. The superfusate collected from naïve donor animals had, in contrast, no effect on synaptic transmission in any of the recipient animals (Fig. 4B). When glial cells were blocked in the recipient animals "transferable LTP" was still induced (to 160 ± 20%, $n = 9$, $P < 0.001$; Fig. 4C). Blockade of interleukin-1β (IL-1β) signaling in the recipient animals also had no effect on the induction of transferable LTP (to 133 ± 12% at 180 – 240 min, $n = 10$, $P = 0.001$; Fig. 4D). However, LTP induction was prevented by blocking TNF (Fig. 4E), D-serine signaling (Fig. 4F) or spinal NMDA receptors (Fig. 4G) in the recipient animals. Application of D-serine to the spinal cord dose-dependently induced a reversible synaptic facilitation (to 152 ± 9% at 220 – 240 min, $n = 10$, $P < 0.001$; fig. S6), while TNF application triggers robust LTP at C-fiber synapses (*21*). These data indicate that transferable LTP required activation of glial cells in the donor, but not in the recipient animals and that the combined actions of the gliotransmitters D-serine and TNF were required for its induction.

Collectively our data indicate that the combined activation of microglia and astrocytes either by $P2X_7R$ agonists or by HFS of primary afferents triggered gliogenic LTP at C-fiber synapses with spinal lamina I neurons via the release of D-serine and cytokines such as TNF. Crucially, glial cell-derived signaling molecules accumulated in the extracellular space including the cerebrospinal fluid at biologically active, but presently unknown concentrations and induced LTP at C-fiber synapses, constituting the phenomenon of gliogenic LTP.

Gliogenic LTP is a new form of paracrine synaptic plasticity in the central nervous system and may lead to pain amplification close to and remote from an injury or an inflammation. This is in line with the concept of chronic pain as a gliopathy involving neurogenic neuroinflammation (*7*, *24*). These new insights may pave the way for novel pain therapies (*25*, *26*). $P2X_7Rs$ play a key role in chronic inflammatory and neuropathic pain (*27*) and in other neurodegenerative and neuropsychiatric disorders (*28*). Glial cells display considerable diversity between and within distinct regions of the CNS (*29*). If the presently identified gliogenic LTP also existed at some brain areas, it could be of relevance not only for pain but also for other disorders such as cognitive deficits, fear and stress disorders, and chronic immune-mediated diseases (*24*, *29*, *30*).

REFERENCES AND NOTES

1. T. V. P. Bliss, G. L. Collingridge, A synaptic model of memory: Long-term potentiation in the hippocampus. *Nature* **361**, 31–39 (1993). Medline doi:10.1038/361031a0
2. H. Ikeda, B. Heinke, R. Ruscheweyh, J. Sandkühler, Synaptic plasticity in spinal lamina I projection neurons that mediate hyperalgesia. *Science* **299**, 1237–1240 (2003). Medline doi:10.1126/science.1080659
3. H. Ikeda, J. Stark, H. Fischer, M. Wagner, R. Drdla, T. Jäger, J. Sandkühler, Synaptic amplifier of inflammatory pain in the spinal dorsal horn. *Science* **312**, 1659–1662 (2006). Medline doi:10.1126/science.1127233
4. R. Kuner, Central mechanisms of pathological pain. *Nat. Med.* **16**, 1258–1266 (2010). Medline doi:10.1038/nm.2231
5. X.-Y. Li, H. G. Ko, T. Chen, G. Descalzi, K. Koga, H. Wang, S. S. Kim, Y. Shang, C. Kwak, S. W. Park, J. Shim, K. Lee, G. L. Collingridge, B. K. Kaang, M. Zhuo, Alleviating neuropathic pain hypersensitivity by inhibiting PKMzeta in the anterior cingulate cortex. *Science* **330**, 1400–1404 (2010). Medline doi:10.1126/science.1191792
6. R. Drdla, M. Gassner, E. Gingl, J. Sandkühler, Induction of synaptic long-term potentiation after opioid withdrawal. *Science* **325**, 207–210 (2009). Medline doi:10.1126/science.1171759
7. R.-R. Ji, T. Berta, M. Nedergaard, Glia and pain: Is chronic pain a gliopathy? *Pain* **154** (Suppl 1), S10–S28 (2013). Medline doi:10.1016/j.pain.2013.06.022
8. S. B. McMahon, M. Malcangio, Current challenges in glia-pain biology. *Neuron* **64**, 46–54 (2009). Medline doi:10.1016/j.neuron.2009.09.033
9. P. M. Grace, M. R. Hutchinson, S. F. Maier, L. R. Watkins, Pathological pain and the neuroimmune interface. *Nat. Rev. Immunol.* **14**, 217–231 (2014). Medline doi:10.1038/nri3621
10. Q.-J. Gong, Y. Y. Li, W. J. Xin, Y. Zang, W. J. Ren, X. H. Wei, Y. Y. Li, T. Zhang, X. G. Liu, ATP induces long-term potentiation of C-fiber-evoked field potentials in spinal dorsal horn: The roles of $P2X_4$ receptors and p38 MAPK in microglia. *Glia* **57**, 583–591 (2009). Medline doi:10.1002/glia.20786
11. H. W. Tao, L. I. Zhang, F. Engert, M. Poo, Emergence of input specificity of LTP during development of retinotectal connections in vivo. *Neuron* **31**, 569–580 (2001). Medline doi:10.1016/S0896-6273(01)00393-2
12. A. K. Clark, D. Gruber-Schoffnegger, R. Drdla-Schutting, K. J. Gerhold, M. Malcangio, J. Sandkühler, Selective activation of microglia facilitates synaptic strength. *J. Neurosci.* **35**, 4552–4570 (2015). Medline doi:10.1523/JNEUROSCI.2061-14.2015
13. J. G. Gu, A. B. MacDermott, Activation of ATP P2X receptors elicits glutamate release from sensory neuron synapses. *Nature* **389**, 749–753 (1997). Medline doi:10.1038/39639
14. Y.-X. Chu, Y. Zhang, Y.-Q. Zhang, Z.-Q. Zhao, Involvement of microglial P2X7 receptors and downstream signaling pathways in long-term potentiation of spinal nociceptive responses. *Brain Behav. Immun.* **24**, 1176–1189 (2010). Medline doi:10.1016/j.bbi.2010.06.001
15. K. Kobayashi, E. Takahashi, Y. Miyagawa, H. Yamanaka, K. Noguchi, Induction of the P2X7 receptor in spinal microglia in a neuropathic pain model. *Neurosci. Lett.* **504**, 57–61 (2011). Medline doi:10.1016/j.neulet.2011.08.058
16. R. Aoyama, Y. Okada, S. Yokota, Y. Yasui, K. Fukuda, Y. Shinozaki, H. Yoshida, M. Nakamura, K. Chiba, Y. Yasui, F. Kato, Y. Toyama, Spatiotemporal and anatomical analyses of P2X receptor-mediated neuronal and glial processing of sensory signals in the rat dorsal horn. *Pain* **152**, 2085–2097 (2011). Medline doi:10.1016/j.pain.2011.05.014
17. W.-J. He, J. Cui, L. Du, Y. D. Zhao, G. Burnstock, H. D. Zhou, H. Z. Ruan, Spinal $P2X(_7)$ receptor mediates microglia activation-induced neuropathic pain in the sciatic nerve injury rat model. *Behav. Brain Res.* **226**, 163–170 (2012). Medline doi:10.1016/j.bbr.2011.09.015
18. C. Ficker, K. Rozmer, E. Kató, R. D. Andó, L. Schumann, U. Krügel, H. Franke, B. Sperlágh, T. Riedel, P. Illes, Astrocyte-neuron interaction in the substantia gelatinosa of the spinal cord dorsal horn via P2X7 receptor-mediated release of glutamate and reactive oxygen species. *Glia* **62**, 1671–1686 (2014). Medline doi:10.1002/glia.22707
19. J. Jung, Y. H. Shin, H. Konishi, S. J. Lee, H. Kiyama, Possible ATP release through lysosomal exocytosis from primary sensory neurons. *Biochem. Biophys. Res. Commun.* **430**, 488–493 (2013). Medline doi:10.1016/j.bbrc.2012.12.009
20. R. D. Fields, Y. Ni, Nonsynaptic communication through ATP release from volume-activated anion channels in axons. *Sci. Signal.* **3**, ra73 (2010). Medline doi:10.1126/scisignal.2001128
21. D. Gruber-Schoffnegger, R. Drdla-Schutting, C. Hönigsperger, G. Wunderbaldinger, M. Gassner, J. Sandkühler, Induction of thermal hyperalgesia and synaptic long-term potentiation in the spinal cord lamina I by TNF-α and IL-1β is mediated by glial cells. *J. Neurosci.* **33**, 6540–6551 (2013). Medline doi:10.1523/JNEUROSCI.5087-12.2013
22. K. J. Sekiguchi, P. Shekhtmeyster, K. Merten, A. Arena, D. Cook, E. Hoffman, A. Ngo, A. Nimmerjahn, Imaging large-scale cellular activity in spinal cord of freely behaving mice. *Nat. Commun.* **7**, 11450 (2016). Medline doi:10.1038/ncomms11450
23. M. Martineau, T. Shi, J. Puyal, A. M. Knolhoff, J. Dulong, B. Gasnier, J. Klingauf, J. V. Sweedler, R. Jahn, J. P. Mothet, Storage and uptake of D-serine into astrocytic synaptic-like vesicles specify gliotransmission. *J. Neurosci.* **33**, 3413–3423 (2013). Medline doi:10.1523/JNEUROSCI.3497-12.2013
24. D. N. Xanthos, J. Sandkühler, Neurogenic neuroinflammation: Inflammatory CNS reactions in response to neuronal activity. *Nat. Rev. Neurosci.* **15**, 43–53 (2014). Medline doi:10.1038/nrn3617
25. R.-R. Ji, Z. Z. Xu, G. Strichartz, C. N. Serhan, Emerging roles of resolvins in the resolution of inflammation and pain. *Trends Neurosci.* **34**, 599–609 (2011). Medline doi:10.1016/j.tins.2011.08.005
26. X.-H. Wei, X. Wei, F. Y. Chen, Y. Zang, W. J. Xin, R. P. Pang, Y. Chen, J. Wang, Y. Y. Li, K. F. Shen, L. J. Zhou, X. G. Liu, The upregulation of translocator protein (18 kDa) promotes recovery from neuropathic pain in rats. *J. Neurosci.* **33**, 1540–1551 (2013). Medline doi:10.1523/JNEUROSCI.0324-12.2013
27. I. P. Chessell, J. P. Hatcher, C. Bountra, A. D. Michel, J. P. Hughes, P. Green, J. Egerton, M. Murfin, J. Richardson, W. L. Peck, C. B. Grahames, M. A. Casula, Y. Yiangou, R. Birch, P. Anand, G. N. Buell, Disruption of the $P2X_7$ purinoceptor gene abolishes chronic inflammatory and neuropathic pain. *Pain* **114**, 386–396 (2005). Medline doi:10.1016/j.pain.2005.01.002
28. A. M. Basso, N. A. Bratcher, R. R. Harris, M. F. Jarvis, M. W. Decker, L. E. Rueter, Behavioral profile of $P2X_7$ receptor knockout mice in animal models of depression and anxiety: Relevance for neuropsychiatric disorders. *Behav. Brain Res.* **198**, 83–90 (2009). Medline doi:10.1016/j.bbr.2008.10.018
29. B. S. Khakh, M. V. Sofroniew, Diversity of astrocyte functions and phenotypes in neural circuits. *Nat. Neurosci.* **18**, 942–952 (2015). Medline doi:10.1038/nn.4043
30. A. Aguzzi, B. A. Barres, M. L. Bennett, Microglia: Scapegoat, saboteur, or something else? *Science* **339**, 156–161 (2013). Medline doi:10.1126/science.1227901
31. B. Heinke, E. Gingl, J. Sandkühler, Multiple targets of μ-opioid receptor-mediated presynaptic inhibition at primary afferent Aδ- and C-fibers. *J. Neurosci.* **31**, 1313–1322 (2011). Medline doi:10.1523/JNEUROSCI.4060-10.2011
32. H. Dodt, M. Eder, A. Frick, W. Zieglgänsberger, Precisely localized LTD in the neocortex revealed by infrared-guided laser stimulation. *Science* **286**, 110–113 (1999). Medline doi:10.1126/science.286.5437.110
33. R. Ruscheweyh, L. Forsthuber, D. Schoffnegger, J. Sandkühler, Modification of classical neurochemical markers in identified primary afferent neurons with Aβ-, Aδ-, and C-fibers after chronic constriction injury in mice. *J. Comp. Neurol.* **502**, 325–336 (2007). Medline doi:10.1002/cne.21311
34. S. D. Honsek, C. Walz, K. W. Kafitz, C. R. Rose, Astrocyte calcium signals at Schaffer collateral to CA1 pyramidal cell synapses correlate with the number of activated synapses but not with synaptic strength. *Hippocampus* **22**, 29–42 (2012). Medline doi:10.1002/hipo.20843
35. R. Drdla-Schutting, J. Benrath, G. Wunderbaldinger, J. Sandkühler, Erasure of a spinal memory trace of pain by a brief, high-dose opioid administration. *Science* **335**, 235–238 (2012). Medline doi:10.1126/science.1211726

ACKNOWLEDGMENTS

This work was supported by grants P 29206-B27 and W1205 from the Austrian Science Fund (FWF) to J.S. We thank L. Czarnecki for laboratory support; B. Heinke and G. Janeselli for technical support. All of the data are archived on servers of the Center for Brain Research, Medical University of Vienna. The

authors declare no conflicts of interest. M.T.K., R.D.-S., and J.S. designed the research. M.T.K., R.D.-S., M.G., S.D.H., and H.L.T. generated and analyzed the data. M.T.K., R.D.-S., and J.S. wrote the paper with input from the other authors.

SUPPLEMENTARY MATERIALS

www.sciencemag.org/cgi/content/full/science.aah5715/DC1
Materials and Methods
Figs. S1 to S6
Movie S1
References (*31*–*35*)

15 July 2016; accepted 1 November 2016
Published online 10 November 2016
10.1126/science.aah5715

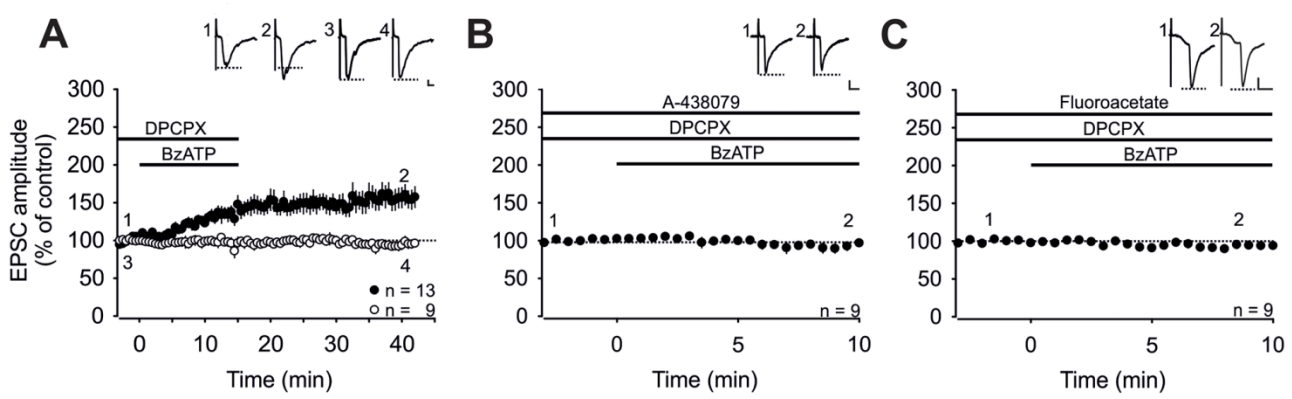

Fig. 1. Activation of spinal $P2X_7$ receptors induces gliogenic LTP at C-fiber synapses. Recordings were performed on lamina I neurons with independent monosynaptic C-fiber inputs from two dorsal root halves. Amplitudes of EPSCs were normalized to 6 baseline values and the mean (±1 SEM) was plotted against time (min). Horizontal bars indicate drug application. (**A**) DPCPX (1 μM) application started at time point –3 min. Bath application of BzATP (100 μM) started at time point 0 min and induced LTP at 13 out of 22 C-fiber inputs (filled circles; $P < 0.001$, at 30 min of wash-out compared to control values). At 9 out of 22 C-fiber inputs, BzATP did not influence EPSC amplitudes (open circles; $P = 0.650$, at 30 min of wash-out compared to control values). (**B**) Bath application of the $P2X_7R$ antagonist A-438079 (10 μM) 13 min prior to BzATP prevented the BzATP-induced LTP at all C-fiber inputs tested ($n = 9$, $P = 0.054$, at 10 min compared to baseline). (**C**) In the presence of fluoroacetate (10 μM), BzATP had no effect on synaptic transmission ($n = 9$, $P = 0.114$ at 10 min compared to baseline). Insets show individual EPSCs at indicated time points. Calibration bars indicate 50 pA and 10 ms. Statistical significance was determined by using RM ANOVA followed by Bonferroni *t* test. Paired *t* test was used for control recordings.

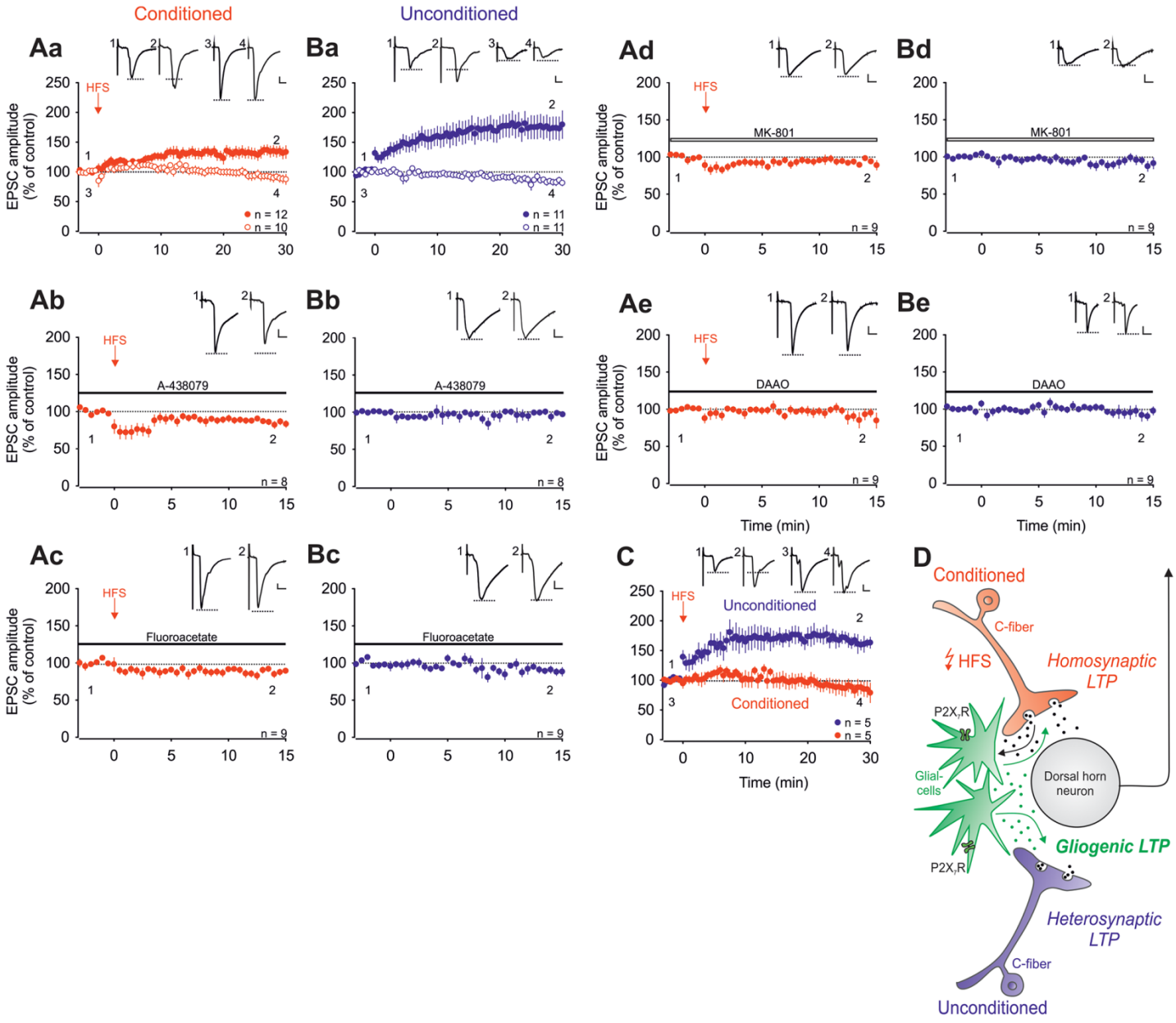

Fig. 2. Homo- and heterosynaptic forms of LTP are induced independently of each other at C-fiber synapses by conditioning HFS. Recordings were performed on lamina I neurons with independent monosynaptic C-fiber inputs from two dorsal root halves. Amplitudes of EPSCs were normalized to 6 baseline values and the mean (±1 SEM) was plotted against time (min). HFS was applied to one dorsal root (arrow; conditioned site in red) at time point 0 min. Horizontal bars indicate drug application. (**Aa**) HFS induced LTP at conditioned synapses in 12 out of 22 neurons (homosynaptic LTP in red, filled circles; $P < 0.001$, at 30 min compared to control values). In 10 of these neurons, no homosynaptic LTP was induced (open circles; $P = 0.105$). (**Ba**) HFS induced LTP at unconditioned synapses in 11 out of the same 22 neurons tested (heterosynaptic LTP in blue, filled circles; $P < 0.001$, at 30 min compared to control values). In 11 of these neurons, no heterosynaptic LTP was observed (open circles; $P = 0.003$). (**C**) In 5 out of these 22 neurons tested, HFS induced LTP at unconditioned (filled circles in blue; 161 ± 10%, $P = 0.005$), but not at conditioned synapses (filled circles in red; $P = 0.313$). (**D**) Schematic illustration of homo- and heterosynaptic forms of LTP as varieties of gliogenic LTP. (**Ab** and **Bb**) HFS failed to induce LTP at the conditioned site in the presence of A-438079 (10 μM; $n = 8$, $P = 0.006$). A-438079 had no effect on EPSC amplitudes at unconditioned synapses. (**Ac** and **Bc**) In the presence of fluoroacetate, LTP induction by HFS was abolished at conditioned and at unconditioned sites (10 μM; $n = 9$, $P = 0.006$ and $P = 0.034$ respectively). (**Ad** to **Be**) The NMDA receptor blocker MK-801, which was added to the pipette solution (1 mM; $n = 9$, open bar; $P = 0.044$ and $P = 0.250$ respectively) or DAAO applied to the bath solution (0.2 $U \cdot ml^{-1}$; $n = 9$, $P = 0.006$ and $P = 0.572$ respectively) blocked the induction of LTP on both sites. Insets show individual EPSC traces recorded at indicated time points. Calibration bars indicate 100 pA and 10 ms. Statistical significance was determined by paired *t* test. In case of non-normality, Wilcoxon signed-rank test was used.

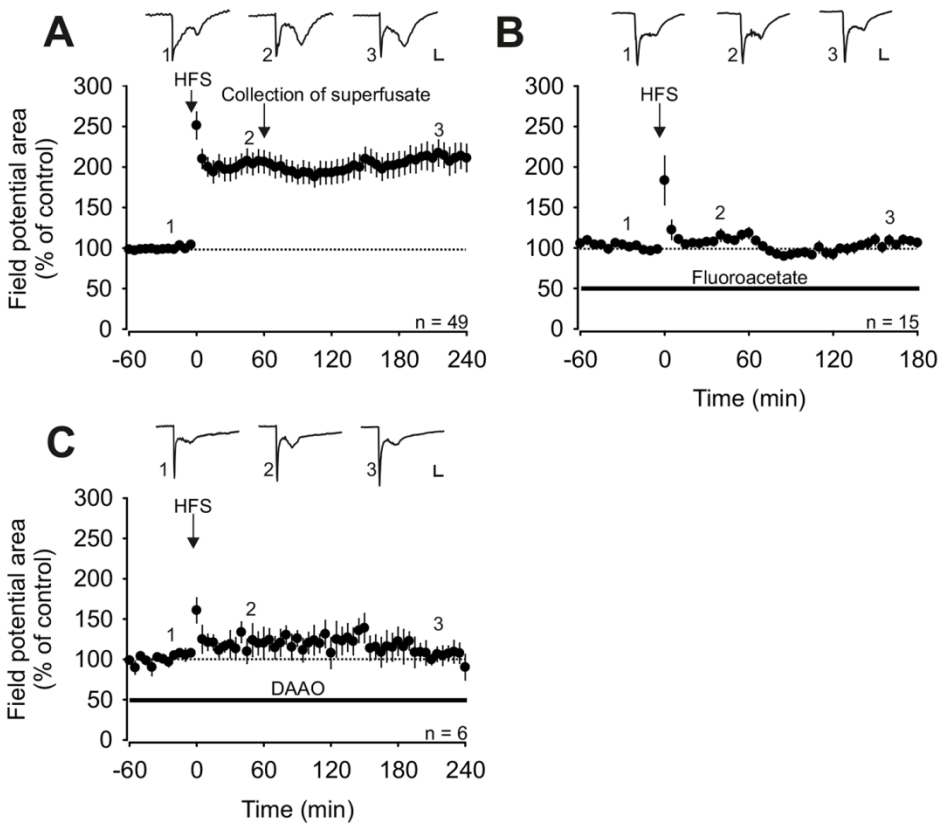

Fig. 3. HFS-induced LTP in vivo depends on spinal glial cells and D-serine signaling. Area of C-fiber-evoked field potentials was normalized to baseline values prior to conditioning HFS and plotted against time (min). Data are expressed as mean ± 1 SEM. Horizontal bars indicate drug application. (**A**) Mean time course of LTP of C-fiber-evoked field potentials. HFS at time point 0 min (arrow) induced LTP in all animals tested (n = 49, P < 0.001). One hour after HFS, the superfusate was collected from the lumbar spinal cord dorsum and transferred to animals shown in Fig. 4. (**B**) Spinal superfusion with the glial inhibitor fluoroacetate (10 μM) fully blocked HFS-induced potentiation in all animals tested (n = 15, P = 0.085). (**C**) HFS-induced LTP was fully prevented by spinal superfusion with DAAO (1 U·ml^{-1}; n = 6, P = 0.365). Insets show original traces of field potentials recorded at indicated time points. Calibration bars indicate 0.2 mV and 50 ms. RM ANOVA on ranks was performed to determine statistical significance in (A). In all other experiments, data were analyzed by using RM ANOVA.

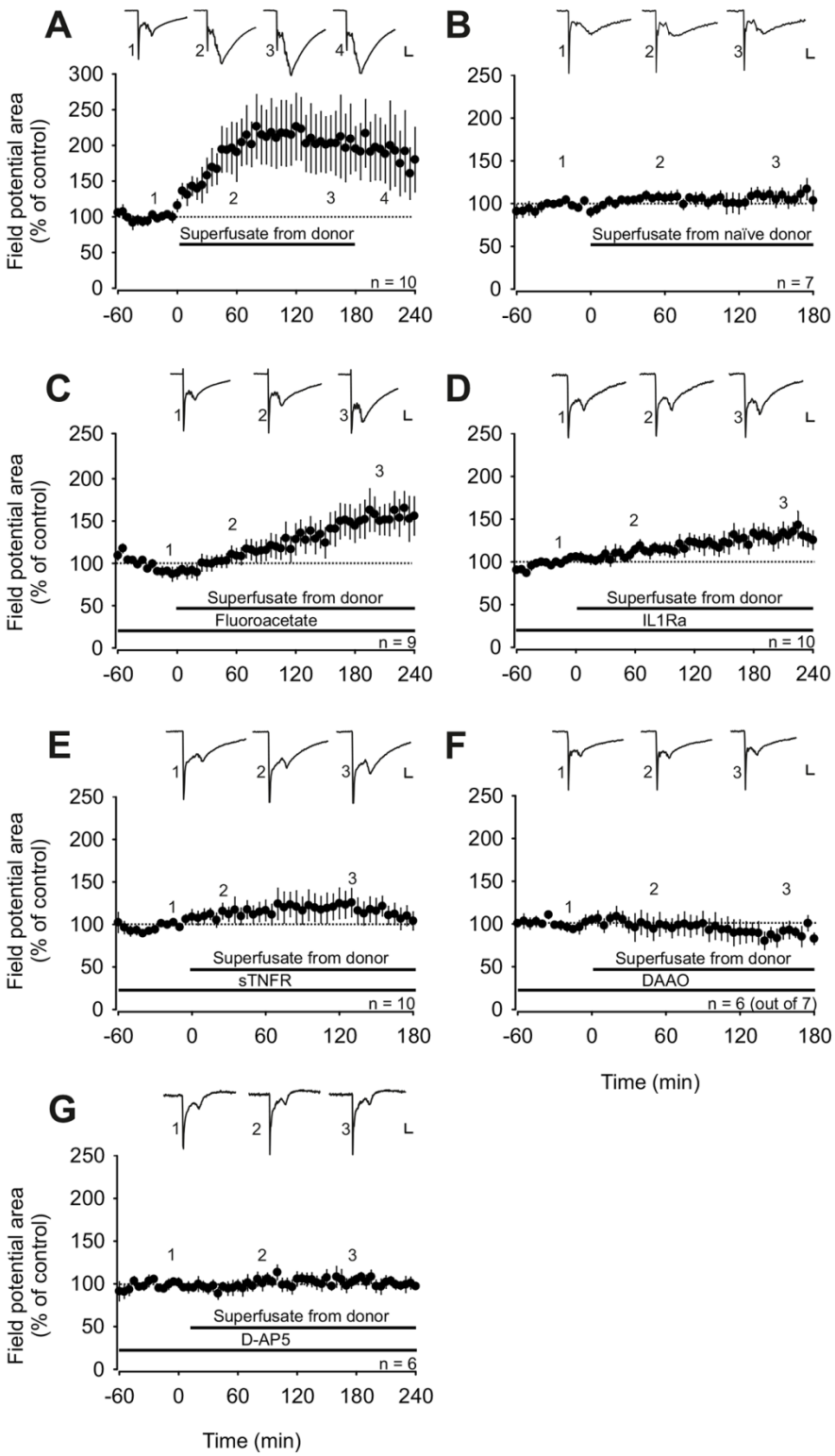

Fig. 4. LTP can be transferred between animals. Area of C-fiber-evoked field potentials was normalized to baseline values prior to transfer of the superfusate and plotted against time (min). Data are expressed as mean ± 1 SEM. Horizontal bars indicate application of superfusate or drugs. (**A**) Spinal application of superfusates collected from donor animals shown in Fig. 3A one hour after HFS induced potentiation of C-fiber-evoked field potentials in all recipient animals tested (n = 10, P = 0.009). (**B**) Superfusates collected from naïve donor animals (no HFS) had no effect on synaptic strength in recipient animals (n = 7, P = 0.477). (**C**) Superfusion of the recipient spinal cord dorsum with fluoroacetate (10 μM) or (**D**) IL1Ra (80 pg·ml^{-1}) did not block LTP induction [n = 9, P < 0.001 in (C) and n = 10, P = 0.001 in (D)]. LTP was, however, blocked by topical application of sTNFR (1 μg·ml^{-1}; n = 10, P = 0.38), DAAO (1 U·ml^{-1}; n = 6 out of 7, P = 0.519) or D-AP5 (100 μM; n = 6, P = 0.652). (**E** to **G**) Insets show original traces of field potentials recorded at indicated time points. Calibration bars indicate 0.2 mV and 50 ms. In (A) data were analyzed using a RM ANOVA on ranks followed by Dunnett's test. In all other experiments, statistical significance was determined by using RM ANOVA.

Gliogenic LTP spreads widely in nociceptive pathways
M. T. Kronschläger, R. Drdla-Schutting, M. Gassner, S. D. Honsek, H. L. Teuchmann and J. Sandkühler (November 10, 2016)
published online November 10, 2016

Editor's Summary

Science (print ISSN 0036-8075; online ISSN 1095-9203) is published weekly, except the last week in December, by the American Association for the Advancement of Science, 1200 New York Avenue NW, Washington, DC 20005.

www.sciencemag.org/cgi/content/full/science.aah5715/DC1

Supplementary Materials for

Gliogenic LTP spreads widely in nociceptive pathways

M. T. Kronschläger, R. Drdla-Schutting, M. Gassner,
S. D. Honsek, H. L. Teuchmann, J. Sandkühler*

*Corresponding author. Email: juergen.sandkuehler@meduniwien.ac.at

Published 10 November 2016 on *Science* First Release
DOI: 10.1126/science.aah5715

This PDF file includes:

Other Supplementary Material for this manuscript includes the following:
(available at www.sciencemag.org/cgi/content/full/science.aah5715/DC1)

Materials and Methods

All experiments were performed in accordance with the European Community's Council directives 2010/63/EU and the rules of the Good Scientific Practice Guide of the Medical University of Vienna. They were approved by the Austrian Federal Ministry for Education, Science and Culture. Animals were fed with a standard diet with access to food and water *ad libitum*.

Spinal cord slice preparation

Under deep isoflurane anesthesia, the lumbar spinal cord was removed from male Sprague-Dawley rats (aged 20 to 25 days) as described previously (*31*). Transverse spinal cord slices (L4 - L6, 500 - 600 µm thick) each with an attached dorsal root (length: 10 - 15 mm) were cut on a microslicer. For the recordings shown in Fig.1, 2 and S4A the dorsal roots of one slice were separated into halves for stimulation of two independent primary afferent inputs. The slices were incubated for 30 min at 32°C and then stored at room temperature (~21°C) in oxygenated incubation solution containing (in mM): 95 NaCl, 1.8 KCl, 1.2 KH_2PO_4, 0.5 $CaCl_2$, 7 $MgSO_4$, 26 $NaHCO_3$, 15 glucose, 50 sucrose, pH was 7.4, measured osmolarity 310 – 320 $mosmol \cdot l^{-1}$.

Electrophysiological recordings *in vitro*

A single slice was transferred to the recording chamber, where it was continuously superfused at a rate of 3 – 4 $ml \cdot min^{-1}$ with oxygenated recording solution. The recording solution was identical to the incubation solution except for (in mM): 127 NaCl, 2.4 $CaCl_2$, 1.3 $MgSO_4$, 0 sucrose.

All recordings were conducted at room temperature. Superficial dorsal horn neurons were visualized with Dodt infrared optics (*32*) using a 40x, 0.80 N.A. water immersion objective on an upright microscope. Lamina I was identified as the area located within a distance of less than 20 µm from the overlying white matter border. Only lamina I neurons were considered for the experiments and recorded in the whole-cell patch clamp configuration with glass pipettes (2 – 4 MΩ) filled with internal solution (in mM): 120 potassium gluconate, 20 KCl, 2 $MgCl_2$, 20 Hepes, 0.5 Na-GTP, 0.5 Na_4-EGTA, 2 Na_2-ATP, 7.5 Phosphocreatine disodium salt hydrate, pH 7.28 adjusted with KOH, measured osmolarity 310 mosmol·l^{-1}. The patch pipettes were pulled on a horizontal micropipette puller from borosilicate glass. Voltage-clamp recordings were made at a holding potential of –70 mV using a patch clamp amplifier and an acquisition software package. Signals were low-pass filtered at 2 – 10 kHz, sampled at 20 kHz and analyzed offline.

Passive membrane properties

The resting membrane potential was measured immediately after establishing the whole-cell configuration. Only neurons with a resting membrane potential more negative than –50 mV were used for further analysis. Membrane resistance, membrane capacitance and series resistance were calculated from the averaged reaction to 20 consecutive hyperpolarizing voltage steps from –70 to –80 mV for 100 ms. Neurons with a calculated series resistance of more than 30 MΩ were excluded from further analysis.

Evoked Excitatory Postsynaptic Currents (EPSCs)

EPSCs were evoked by stimulating dorsal root afferents using a suction electrode with an isolated current stimulator. After determining the threshold value to elicit an EPSC, two consecutive pulses (0.1 ms pulse width, 300 ms time interval) were given at 15 s intervals. In slices where the dorsal roots were divided into halves, test stimuli were applied at 15 s intervals alternatively to one half. The intensity for test stimuli was set to 200% of the threshold value. Afferent input was classified as being C-fiber-evoked based on a combination of response threshold of > 1 mA and conduction velocity of < 1 $m \cdot s^{-1}$(*33*). C-fiber-evoked EPSCs were considered monosynaptic by the absence of failures during 10 consecutive pulses at 2 Hz and a jitter in response latencies lower than 10%. Only neurons fulfilling all these criteria were further analyzed. Series resistance was monitored throughout the recording by applying a square pulse of –10 mV for 10 ms at 15 s intervals. Neurons were discarded when the series resistance changed by more than 20% during the experiment. For every cell measured, we performed a paired t-test to evaluate whether EPSC amplitude at the end of the recording was significantly different from baseline. In addition, a minimum increase in EPSC amplitude of 10% was required to be considered a responder.

For LTP induction, conditioning high-frequency stimulation (HFS, 3 x 100 Hz for 1 s at 10 s intervals) was applied at 5 mA to the dorsal root or to one dorsal root half (conditioned input). Holding currents were set to zero during conditioning stimulation.

NPE-IP_3 uncaging and calcium imaging in astrocytes

Experiments were performed at room temperature in normal oxygenated recording solution. For UV-light-triggered rise in intracellular calcium ion concentration, astrocytic

networks were filled via patch-pipettes (3 – 6 MΩ resistance) as described previously (*34*). In brief, patch-pipettes were filled with an intracellular solution consisting of the following (in mM): 120 potassium gluconate, 20 KCl, 2 $MgCl_2$, 20 Hepes, 0.5 Na-GTP, 2 Na_2-ATP, 7.5 Phosphocreatine disodium salt hydrate, 0.4 F5F (to monitor intracellular calcium increases), 2 NPE-caged IP_3 (to induce the release of calcium from intracellular stores) as well as 0.01% sulforhodamine B (SRB, to visualize the network extension). For control recordings, NPE-caged IP_3 was omitted from the intracellular solution. After establishing the whole-cell configuration, electrophysiological properties were determined with an amplifier coupled to a digitizer and the pClamp10 software package. After confirming that recorded cells exhibited electrophysiological characteristics of astrocytes (low input resistance, linear current-voltage relationship, membrane potential more negative than –70 mV), the astrocytic network was filled for at least 30 min. After successful withdrawal of the patch pipette, a lamina I neuron with the cell body within the area of the filled astrocytic network was patched. Neuronal recordings were performed and analyzed as described above.

Uncaging of NPE-caged IP_3 in the astrocytic network was induced by UV-flashes applied via an optical fiber (365 µm diameter, N.A. 0.22) coupled to a computer-controlled Xenon-Flashlamp system (settings C3/300 V). UV-light was band-pass (270 – 400 nm) and long-pass filtered (295 nm). UV-pulse trains consisted of three stimulations at 10 s intervals, during which 5 UV-flashes were applied at 5 Hz (i.e. 1 s stimulation at 15 s, 26 s and 37 s).

Calcium-imaging was performed via multiphoton imaging on a microscope equipped with a 20x objective (N.A. 1.0) and a Chameleon-XR Ti-sapphire laser. SRB and F5F

were excited at 820 nm, and fluorescence emission was collected with non-descanned detectors (NDDs) at 565 – 605 nm and 500 – 550 nm, respectively. Images were collected at 2 Hz for 60 s. Data were collected from somata of F5F-filled astrocytes in a single optical plane, located at the same level as the recorded lamina I neuron. Data are expressed as changes in fluorescence intensity relative to baseline fluorescence ($\Delta F/F$).

Animal surgery for *in vivo* experiments

Experiments were performed on male Sprague-Dawley rats weighing between 150 and 250 g. Isoflurane (4 vol%) in two thirds N_2O and one third O_2 was initially administered via a respiratory mask to induce anesthesia. Animals were intubated using a 16 G cannula and then mechanically ventilated at a rate of 75 strokes·min^{-1} using a tidal volume of 4 – 6 ml. Anesthesia was maintained by 1.5 vol% isoflurane. Body core temperature was kept at 37.5°C with a feedback controlled heating blanket. Deep surgical level of anesthesia was verified by stable mean arterial blood pressure during noxious stimulation. Surgical procedures were performed as described previously (*35*). Briefly, a jugular vein and a carotid artery were cannulated to allow intravenous (i.v.) infusions and arterial blood pressure monitoring, respectively. Muscle relaxation was achieved by 2 μg·kg $^{-1}$·h $^{-1}$ i.v. pancuronium bromide. Following cannulation, the left sciatic nerve was dissected free for bipolar electrical stimulation with a silver hook electrode. The lumbar segments L4 and L5 were exposed by laminectomy. The dura mater was carefully incised and retracted. Two metal clamps were used for fixation of the vertebral column in a stereotactic frame. An agarose pool was formed around the exposed spinal segments. The spinal cord was continuously superfused with 5 ml artificial cerebrospinal fluid consisting of (in mM): 135 NaCl, 1.7 KCl, 1.8 $CaCl_2$, 10 HEPES, 1 $MgCl_2$, pH 7.4 adjusted with KOH,

measured osmolarity 290 mosmol·l^{-1} by means of a roller pump in a closed circuit system, in which additional drugs could be dissolved as indicated. For transfer experiments, the total volume of the superfusate (i.e. 5 ml) was collected from a donor animal one hour after conditioning HFS (or after one hour of baseline recordings for control recordings) and transferred to a recipient animal by replacing the superfusate circulating during baseline recording. At the end of each electrophysiological experiment, animals were decapitated under deep anesthesia. The spinal cord was removed and cryo-fixed for detection of a rhodamine B spot at the recording site under a fluorescence microscope. Only those experiments where the recording site was located in laminae I or II were analyzed further.

Electrophysiological recordings *in vivo*

Electrophysiological recordings were performed as described previously (*35*). Briefly, C-fiber-evoked field potentials were recorded with glass electrodes (impedance 2 – 3 MΩ) from laminae I and II of the spinal cord dorsal horn in response to stimulation of sciatic nerve fibers at C-fiber strength. The pipette solution consisted of 135 mM NaCl, 1.7 mM KCl, 1.8 mM $CaCl_2$, 10 mM Hepes, 1 mM $MgCl_2$ and 0.2% rhodamine B. At the end of each electrophysiological experiment the recording site was labelled by pressure application (300 mbar for 1 min) with 0.2% rhodamine B via the electrode. Electrodes were driven by a microstepping motor. Recordings were made with an amplifier using a band width filter of 0.1 – 1000 Hz. Signals were monitored on a digital oscilloscope and digitized by an A/D converter. Test stimuli were delivered to the sciatic nerve and consisted of pulses of 0.5 ms duration at 25 V applied every 5 min using an electrical

stimulator. LTP was induced by electrical HFS (four trains of 100 Hz, 60 V, 0.5 ms pulses for 1 s at 10 s intervals).

Drugs and drug administration

For *in vitro* recordings, all substances were added to the recording solution or to the intracellular solution at known concentrations as indicated. Drugs used were sulforhodamine B (SRB; 0.01%), 2′ (3′)-O-(4-Benzoylbenzoyl) adenosine 5′-triphosphate triethylammonium salt (BzATP, 100 µM), A-438079 (10 µM), Na-fluoroacetate (10 µM), catalase (300 $U \cdot ml^{-1}$), D-amino acid oxidase (DAAO, 0.2 $U \cdot ml^{-1}$), D-2-amino-5-phosphonopentanoate (D-AP5, 50 µM), D-myo-inositol trisphosphate-P4-1-(2-Nitrophenyl)ethyl-ester (NPE-caged IP_3, 2 mM, [cag-0-145]), Fluo-5F (400 µM), MK-801 maleate (1 mM), 8-Cyclopentyl-1, 3-dipropylxanthine (DPCPX, 1 µM) and D-serine (100 µM). Slices were pre-incubated in fluoroacetate for recordings shown in Fig. 1C, 2Ac, 2Bc and S1E, and in DAAO and catalase for recordings shown in 2Ae and 2Be for at least 1 h before use. All other drugs were applied to a closed system of 10 or 20 ml recording solution.

For *in vivo* recordings, pancuronium bromide was administered as an i.v. infusion (2 $\mu g \cdot kg^{-1} \cdot h^{-1}$). All other drugs were dissolved in distilled water and added directly to a closed system of 5 ml artificial cerebrospinal fluid superfusate to obtain the desired concentration as indicated: Na-fluoroacetate (10 µM), DAAO ($1U \cdot ml^{-1}$), D-serine (10 µM or 100 µM), D-AP5 (100 µM), the interleukin 1 receptor antagonist IL1-Ra (80 $pg \cdot ml^{-1}$) and the soluble TNF receptor (sTNFR; 1 $\mu g \cdot ml^{-1}$).

Statistical Analysis

C-fiber-evoked EPSCs were analyzed offline using pClamp10 and SigmaPlot12. For quantification of synaptic strength the peak amplitude of the evoked EPSCs was measured. The mean amplitude of 6 evoked EPSCs prior to substance application or conditioning stimulation served as control and was compared to the mean amplitude of 6 EPSCs at different time points within the recording as indicated in the figure legends (e.g. 0 – 3 min, 2 – 5 min, 7 – 10 min, 12 – 15 min, 17 – 20 min, 27 – 30 min). Data were tested for normality (Shapiro-Wilk test) and for equal variance. Statistical significance was tested with a one-way repeated measures analysis of variance (RM ANOVA) with Bonferroni post-hoc correction or with a paired t-test. In case normality failed, a Wilcoxon signed-rank test was performed. The critical value for statistical significance was set at $P < 0.05$. Values are presented as mean ± 1 standard error of mean (SEM).

C-fiber-evoked field potentials were analyzed offline using pClamp10 and SigmaPlot12. For quantification, the area under the curve of C-fiber-evoked field potentials was determined. The mean area under the curve of 5 consecutive stable field potentials prior to conditioning stimulation, or application of the superfusates from donor animals in case of transfer-experiments, served as baseline control. Responses were normalized to the baseline in every animal. Data were tested for normality using the Shapiro-Wilk test. Unless otherwise indicated, RM ANOVA was performed to compare the different experimental protocols and treatments. In all experimental groups, baseline was compared to different time points during the recording (40 – 60 min, 160 – 180 min and 220 – 240 min, and 280 – 300 min in Fig. S6, respectively). ANOVA was followed by Bonferroni post-hoc correction. Nonparametric one-way RM ANOVA on ranks was

performed in the case of non-normality. RM ANOVA on ranks was corrected by Dunnett´s test. The critical value for statistical significance was set at $P < 0.05$. Values are expressed as mean ± 1 SEM.

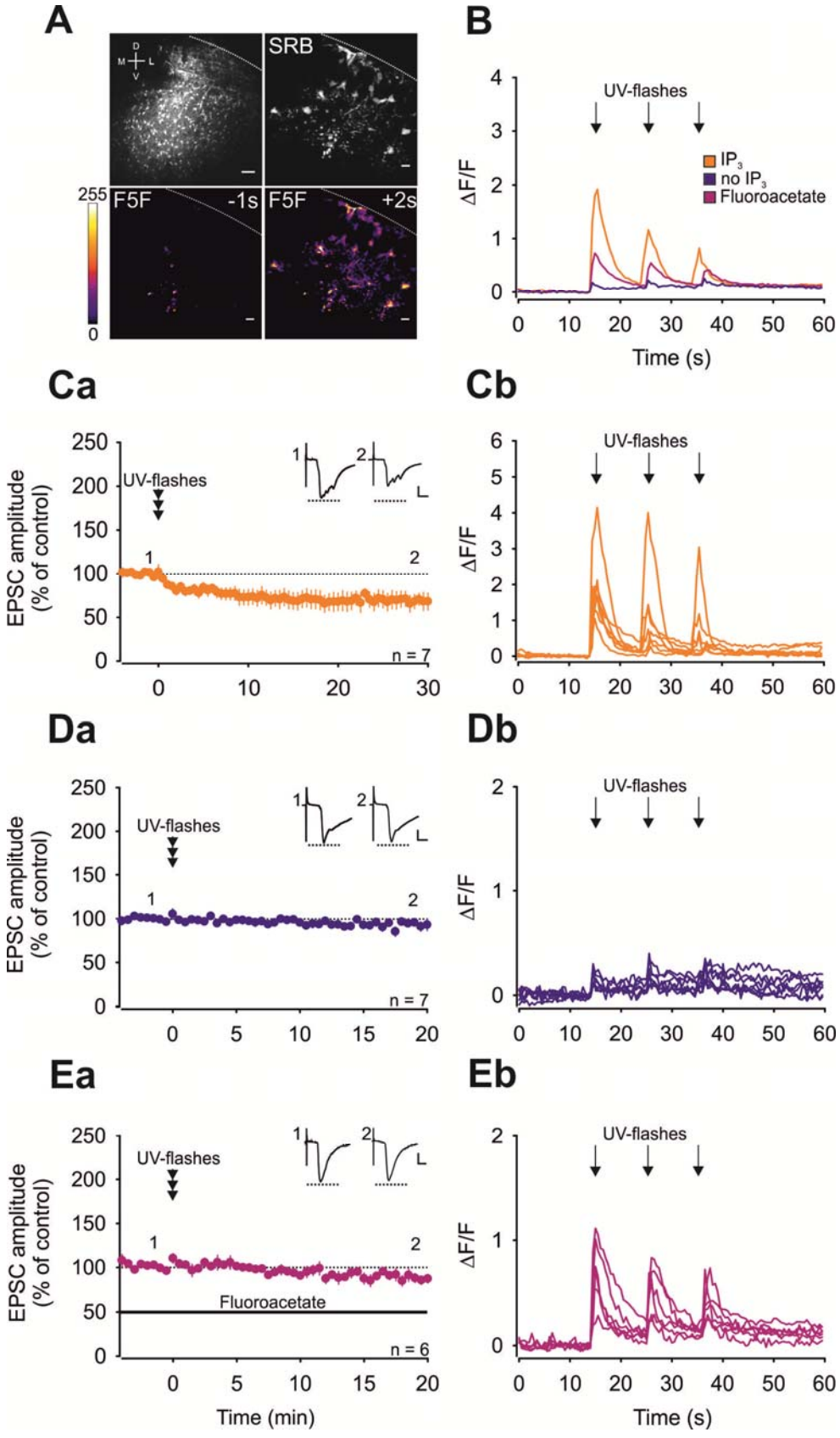
A
SRB
255
F5F -1s
F5F +2s
0
B
UV-flashes
IP3
no IP3
Fluoroacetate
ΔF/F
Time (s)
Ca
EPSC amplitude (% of control)
UV-flashes
n = 7
Cb
Da
n = 7
Db
Ea
Fluoroacetate
n = 6
Time (min)
Eb

Fig. S1. Gliogenic LTD is induced at C-fiber synapses after IP_3 uncaging in astrocytic networks. (**A**) Dye coupling of astrocytes in the spinal dorsal horn. The white dotted lines mark the dorsal borders of the slices. Uncaging of IP_3 (2 mM) by application of UV-flashes (5 Hz, 3 x 1 s at 10 sec interval) induced an increase in $[Ca^{2+}]_i$ in astrocytes. The Fluo-5F (F5F) images are pseudo colored to indicate changes in F5F fluorescence intensity upon IP_3 uncaging. Calibration bars indicate 50 μm (top left) or 10 μm, respectively. (**B**) Mean change in F5F fluorescence intensity of astrocytes (ΔF/F) in response to UV-flashes under three different conditions: IP_3 uncaging (orange trace**; Cb)**, UV-flash application where IP_3 was omitted (purple trace**; Db**) and IP_3 uncaging under fluoroacetate (magenta trace; **Eb**). (**Ca-Ea**) EPSC recordings from lamina I neurons with monosynaptic C-fiber input lying within the areas of the astrocytic networks tested. Amplitudes of individual EPSCs were normalized to 6 baseline values and the mean (± 1 SEM) was plotted against time (min). (**Ca**) IP_3 uncaging in astrocytes induced LTD at C-fiber synapses (n = 7, P = 0.001, 30 min after UV-flashes compared to baseline). (**Da**) In the absence of caged IP_3, UV-flashes do not affect synaptic strength (n = 7, P = 0.061, 20 min after UV-flashes compared to baseline). (**Ea**) In the presence of fluoroacetate (10 μM), uncaging of IP_3 had no effect on synaptic transmission (n = 6, P = 0.112, 20 min after UV-flashes compared to baseline). During UV-flashes, holding currents were set to 0. Insets show individual EPSCs recorded at indicated time points. Calibration bars indicate 200 pA and 10 ms. Statistical significance was determined by using one-way repeated measures analysis of variance (RM ANOVA) followed by Bonferroni t-test. Paired t-test was used for control recordings.

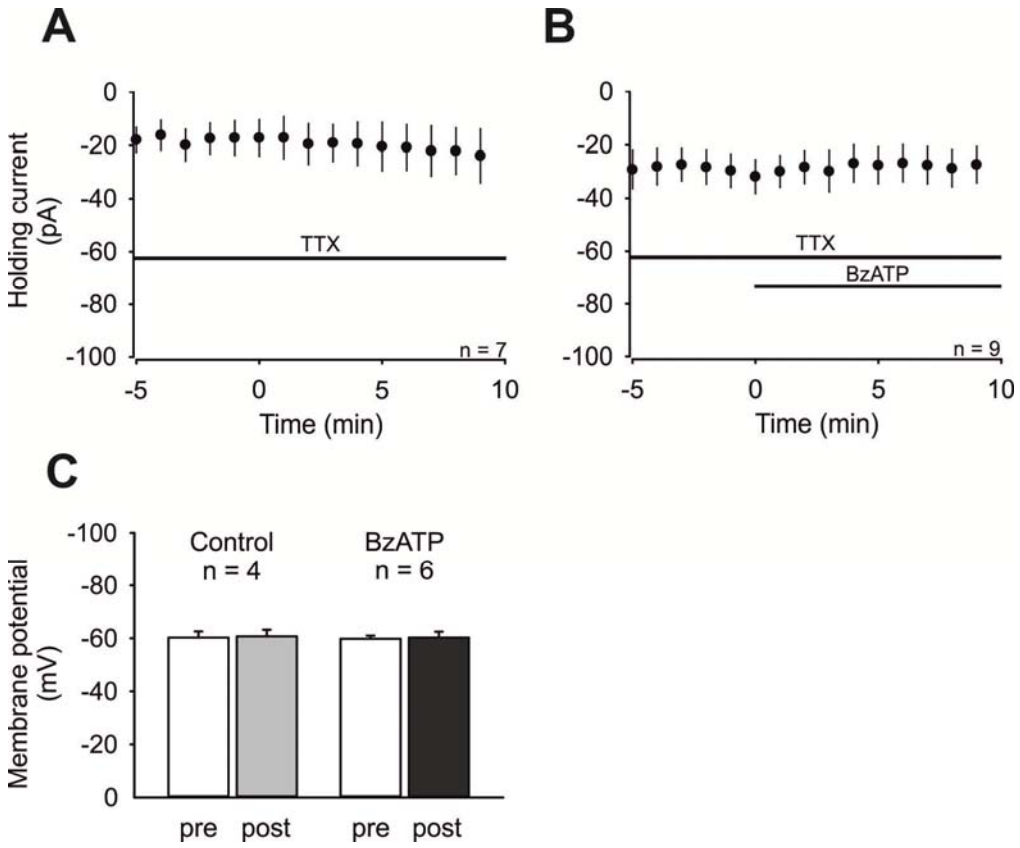

Fig. S2. Membrane properties of lamina I neurons are not changed by bath application of a P2X$_7$R agonist. Holding current and membrane potential recordings were performed on lamina I neurons. TTX (1 μM) was bath-applied at least 3 min prior to recording. Data are expressed as mean ± 1 SEM. Horizontal bars indicate drug application. (**A**) Holding current analysis of recorded neurons during TTX did not reveal any significant change over time (n = 7, P = 0.345 at 9 min compared to control values). (**B**) In the presence of TTX, BzATP (100 μM) application starting at time point 0 min had no effect on holding currents (n = 9, P = 0.556 at 9 min compared to control values). (**C**) Membrane potential recordings in the presence of TTX were stable over time (grey

bar; n = 4, P = 0.516 at 10 min compared to baseline). BzATP (100 μM) was bath applied at time point 0 min and had no effect on the membrane potential (black bar; n = 6, P = 0.851 at 10 min compared to control values). In all experiments, statistical significance was determined by using a paired t-test.

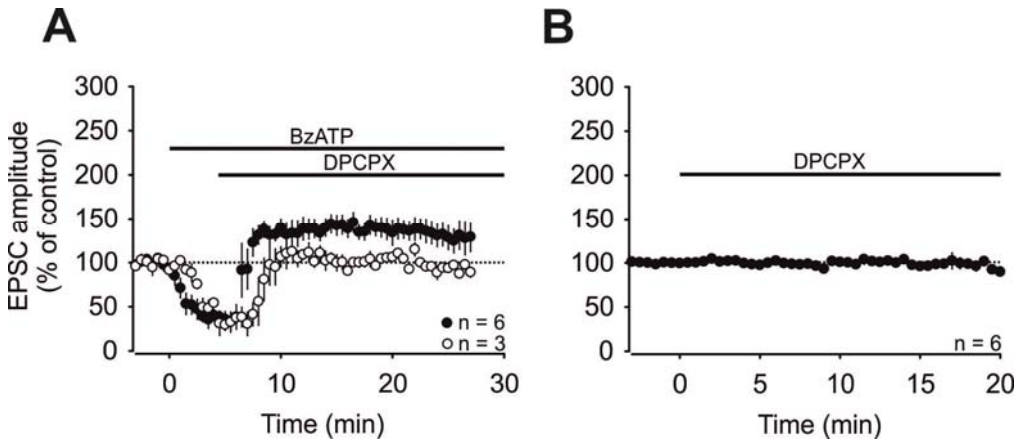

Fig. S3. Blockade of A_1 receptor signaling unmasks $P2X_7R$-mediated potentiation. Recordings were performed on lamina I neurons with monosynaptic C-fiber input. Amplitudes of individual C-fiber-evoked EPSCs were normalized to 6 control values and the mean (± 1 SEM) was plotted against time (min). Horizontal bars indicate drug application. (**A**) Bath application of BzATP induced a significant depression of EPSC amplitudes at all C-fiber synapses tested (filled and open circles; n = 9, $P < 0.001$, 5 min after BzATP application compared to baseline). Blockade of A_1 receptors by DPCPX after BzATP application unveiled a $P2X_7R$-mediated potentiation of synaptic transmission in 6 out of 9 neurons (filled circles; $P = 0.003$, after 10 min of DPCPX application compared with control). In the remaining 3 neurons, blockade of A_1 receptor signaling reversed the BzATP-mediated depression to control values without inducing synaptic potentiation (open circles; $P = 1.0$, after 10 min of DPCPX application compared with control). (**B**) Blockade of A_1 receptor signaling with DPCPX alone had no significant effect on synaptic transmission at any of the C-fiber inputs tested (n = 6, $P = 0.853$, 20 min after DPCPX compared to baseline). Statistical significance was determined by using RM ANOVA followed by Bonferroni t-test. Paired t-test was used for control recordings.

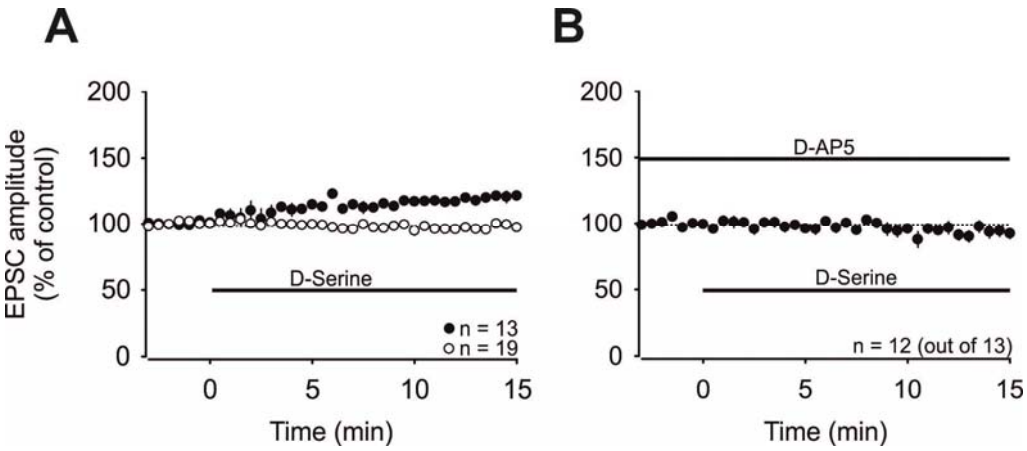

Fig. S4. D-Serine facilitates synaptic strength at spinal C-fiber synapses *in vitro*.

Recordings were performed on lamina I neurons with one (B) or two monosynaptic C-fiber inputs (A). Amplitudes of individual C-fiber-evoked EPSCs were normalized to 6 control values and the mean values (± 1 SEM) were plotted against time (min). Horizontal bars indicate drug application. (**A**) D-Serine (100 μM) added to the bath solution at time point 0 min induced amplification of synaptic strength at 13 out of 32 inputs tested (black circles; $P < 0.001$). In the remaining 19 inputs, D-serine failed to induce potentiation (open circles; $P = 0.04$). (**B**) In the presence of D-AP5 (50 μM), bath application of D-serine had no effect on synaptic strength (n = 12 out of 13, $P = 0.094$, 15 min after D-serine compared to baseline). Statistical significance was determined by using paired t-test.

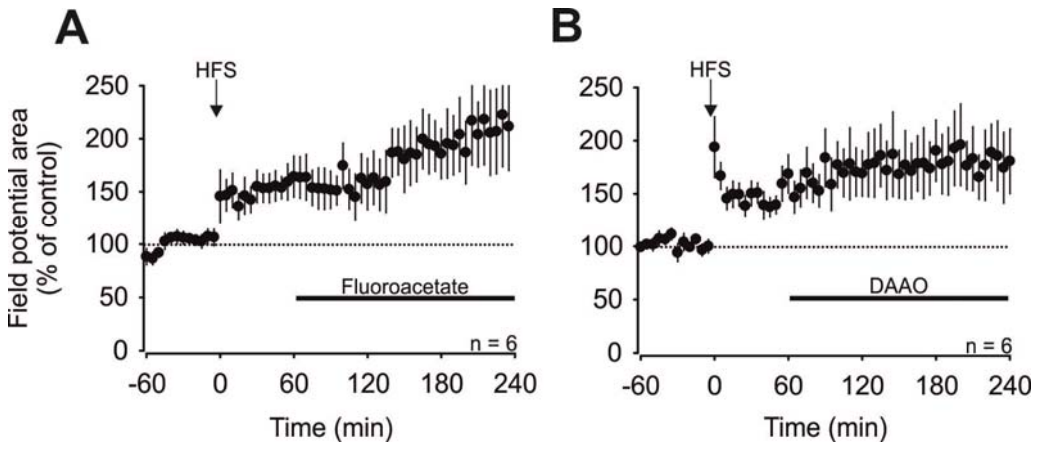

Fig. S5. Maintenance of HFS-induced LTP is not affected by inhibition of glial cell metabolism or by degradation of D-serine. Areas of C-fiber-evoked field potentials were normalized to baseline values and plotted against time (min). Data are expressed as mean ± 1 SEM. LTP was induced by HFS at time point 0 min (arrow). Horizontal bars indicate drug application. (**A**) Spinal superfusion with the glial cell inhibitor fluoroacetate (10 μM) had no effect on LTP maintenance throughout the recording period of 240 min (n = 6, $P = 0.433$). (**B**) Degradation of D-serine with DAAO (1 U·ml^{-1}) did not affect maintenance of HFS-induced LTP (n = 6, $P = 0.546$). Statistical significance was determined by using RM ANOVA followed by Bonferroni t-test.

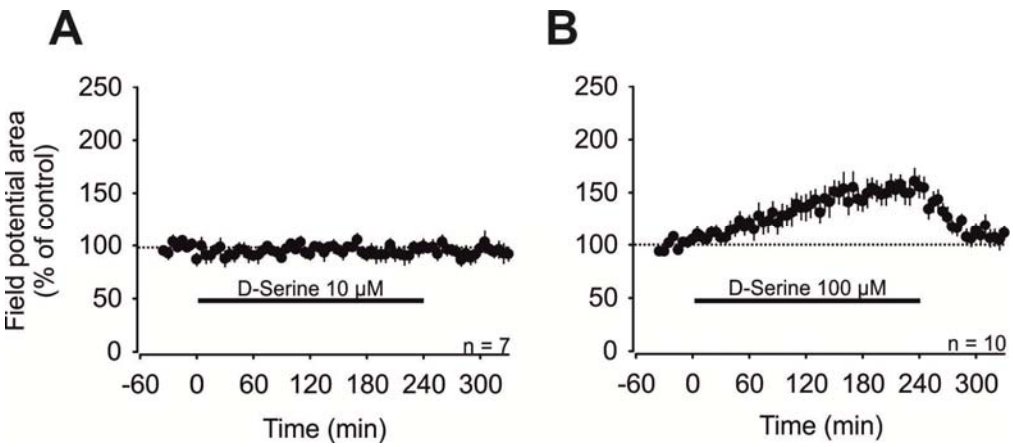

Fig. S6. D-Serine dose-dependently facilitates synaptic strength at spinal C-fiber synapses. Areas of C-fiber evoked field potentials were normalized to baseline values and plotted against time (min). Data are expressed as mean ± 1 SEM. Horizontal bars indicate drug application. (**A**) D-Serine (10 µM), which was added to the superfusate at time point 0 min for four hours had no effect on synaptic strength at C-fiber synapses (n = 7, $P = 0.510$). (**B**) A 10-fold higher concentration of D-serine (100 µM) induced a steadily rising facilitation of synaptic strength ($P < 0.001$). Upon wash-out of D-serine, C-fiber mediated responses returned to baseline levels (n = 10, $P = 0.479$). Statistical significance was determined by using RM ANOVA on ranks followed by Dunnett´s test.

Movie S1

NPE-IP_3 uncaging in spinal astrocytes upon UV-flash application.

References

1. T. V. P. Bliss, G. L. Collingridge, A synaptic model of memory: Long-term potentiation in the hippocampus. *Nature* **361**, 31–39 (1993). Medline doi:10.1038/361031a0

2. H. Ikeda, B. Heinke, R. Ruscheweyh, J. Sandkühler, Synaptic plasticity in spinal lamina I projection neurons that mediate hyperalgesia. *Science* **299**, 1237–1240 (2003). Medline doi:10.1126/science.1080659

3. H. Ikeda, J. Stark, H. Fischer, M. Wagner, R. Drdla, T. Jäger, J. Sandkühler, Synaptic amplifier of inflammatory pain in the spinal dorsal horn. *Science* **312**, 1659–1662 (2006). Medline doi:10.1126/science.1127233

4. R. Kuner, Central mechanisms of pathological pain. *Nat. Med.* **16**, 1258–1266 (2010). Medline doi:10.1038/nm.2231

5. X.-Y. Li, H. G. Ko, T. Chen, G. Descalzi, K. Koga, H. Wang, S. S. Kim, Y. Shang, C. Kwak, S. W. Park, J. Shim, K. Lee, G. L. Collingridge, B. K. Kaang, M. Zhuo, Alleviating neuropathic pain hypersensitivity by inhibiting PKMzeta in the anterior cingulate cortex. *Science* **330**, 1400–1404 (2010). Medline doi:10.1126/science.1191792

6. R. Drdla, M. Gassner, E. Gingl, J. Sandkühler, Induction of synaptic long-term potentiation after opioid withdrawal. *Science* **325**, 207–210 (2009). Medline doi:10.1126/science.1171759

7. R.-R. Ji, T. Berta, M. Nedergaard, Glia and pain: Is chronic pain a gliopathy? *Pain* **154** (Suppl 1), S10–S28 (2013). Medline doi:10.1016/j.pain.2013.06.022

8. S. B. McMahon, M. Malcangio, Current challenges in glia-pain biology. *Neuron* **64**, 46–54 (2009). Medline doi:10.1016/j.neuron.2009.09.033

9. P. M. Grace, M. R. Hutchinson, S. F. Maier, L. R. Watkins, Pathological pain and the neuroimmune interface. *Nat. Rev. Immunol.* **14**, 217–231 (2014). Medline doi:10.1038/nri3621

10. Q.-J. Gong, Y. Y. Li, W. J. Xin, Y. Zang, W. J. Ren, X. H. Wei, Y. Y. Li, T. Zhang, X. G. Liu, ATP induces long-term potentiation of C-fiber-evoked field potentials in spinal dorsal horn: The roles of $P2X_4$ receptors and p38 MAPK in microglia. *Glia* **57**, 583–591 (2009). Medline doi:10.1002/glia.20786

11. H. W. Tao, L. I. Zhang, F. Engert, M. Poo, Emergence of input specificity of LTP during development of retinotectal connections in vivo. *Neuron* **31**, 569–580 (2001). Medline doi:10.1016/S0896-6273(01)00393-2

12. A. K. Clark, D. Gruber-Schoffnegger, R. Drdla-Schutting, K. J. Gerhold, M. Malcangio, J. Sandkühler, Selective activation of microglia facilitates synaptic strength. *J. Neurosci.* **35**, 4552–4570 (2015). Medline doi:10.1523/JNEUROSCI.2061-14.2015

13. J. G. Gu, A. B. MacDermott, Activation of ATP P2X receptors elicits glutamate release from sensory neuron synapses. *Nature* **389**, 749–753 (1997). Medline doi:10.1038/39639

14. Y.-X. Chu, Y. Zhang, Y.-Q. Zhang, Z.-Q. Zhao, Involvement of microglial P2X7 receptors and downstream signaling pathways in long-term potentiation of spinal nociceptive

responses. *Brain Behav. Immun.* **24**, 1176–1189 (2010). Medline doi:10.1016/j.bbi.2010.06.001

15. K. Kobayashi, E. Takahashi, Y. Miyagawa, H. Yamanaka, K. Noguchi, Induction of the P2X7 receptor in spinal microglia in a neuropathic pain model. *Neurosci. Lett.* **504**, 57–61 (2011). Medline doi:10.1016/j.neulet.2011.08.058

16. R. Aoyama, Y. Okada, S. Yokota, Y. Yasui, K. Fukuda, Y. Shinozaki, H. Yoshida, M. Nakamura, K. Chiba, Y. Yasui, F. Kato, Y. Toyama, Spatiotemporal and anatomical analyses of P2X receptor-mediated neuronal and glial processing of sensory signals in the rat dorsal horn. *Pain* **152**, 2085–2097 (2011). Medline doi:10.1016/j.pain.2011.05.014

17. W.-J. He, J. Cui, L. Du, Y. D. Zhao, G. Burnstock, H. D. Zhou, H. Z. Ruan, Spinal P2X($_7$) receptor mediates microglia activation-induced neuropathic pain in the sciatic nerve injury rat model. *Behav. Brain Res.* **226**, 163–170 (2012). Medline doi:10.1016/j.bbr.2011.09.015

18. C. Ficker, K. Rozmer, E. Kató, R. D. Andó, L. Schumann, U. Krügel, H. Franke, B. Sperlágh, T. Riedel, P. Illes, Astrocyte-neuron interaction in the substantia gelatinosa of the spinal cord dorsal horn via P2X7 receptor-mediated release of glutamate and reactive oxygen species. *Glia* **62**, 1671–1686 (2014). Medline doi:10.1002/glia.22707

19. J. Jung, Y. H. Shin, H. Konishi, S. J. Lee, H. Kiyama, Possible ATP release through lysosomal exocytosis from primary sensory neurons. *Biochem. Biophys. Res. Commun.* **430**, 488–493 (2013). Medline doi:10.1016/j.bbrc.2012.12.009

20. R. D. Fields, Y. Ni, Nonsynaptic communication through ATP release from volume-activated anion channels in axons. *Sci. Signal.* **3**, ra73 (2010). Medline doi:10.1126/scisignal.2001128

21. D. Gruber-Schoffnegger, R. Drdla-Schutting, C. Hönigsperger, G. Wunderbaldinger, M. Gassner, J. Sandkühler, Induction of thermal hyperalgesia and synaptic long-term potentiation in the spinal cord lamina I by TNF-α and IL-1β is mediated by glial cells. *J. Neurosci.* **33**, 6540–6551 (2013). Medline doi:10.1523/JNEUROSCI.5087-12.2013

22. K. J. Sekiguchi, P. Shekhtmeyster, K. Merten, A. Arena, D. Cook, E. Hoffman, A. Ngo, A. Nimmerjahn, Imaging large-scale cellular activity in spinal cord of freely behaving mice. *Nat. Commun.* **7**, 11450 (2016). Medline doi:10.1038/ncomms11450

23. M. Martineau, T. Shi, J. Puyal, A. M. Knolhoff, J. Dulong, B. Gasnier, J. Klingauf, J. V. Sweedler, R. Jahn, J. P. Mothet, Storage and uptake of D-serine into astrocytic synaptic-like vesicles specify gliotransmission. *J. Neurosci.* **33**, 3413–3423 (2013). Medline doi:10.1523/JNEUROSCI.3497-12.2013

24. D. N. Xanthos, J. Sandkühler, Neurogenic neuroinflammation: Inflammatory CNS reactions in response to neuronal activity. *Nat. Rev. Neurosci.* **15**, 43–53 (2014). Medline doi:10.1038/nrn3617

25. R.-R. Ji, Z. Z. Xu, G. Strichartz, C. N. Serhan, Emerging roles of resolvins in the resolution of inflammation and pain. *Trends Neurosci.* **34**, 599–609 (2011). Medline doi:10.1016/j.tins.2011.08.005

26. X.-H. Wei, X. Wei, F. Y. Chen, Y. Zang, W. J. Xin, R. P. Pang, Y. Chen, J. Wang, Y. Y. Li, K. F. Shen, L. J. Zhou, X. G. Liu, The upregulation of translocator protein (18 kDa)

promotes recovery from neuropathic pain in rats. *J. Neurosci.* **33**, 1540–1551 (2013). Medline doi:10.1523/JNEUROSCI.0324-12.2013

27. I. P. Chessell, J. P. Hatcher, C. Bountra, A. D. Michel, J. P. Hughes, P. Green, J. Egerton, M. Murfin, J. Richardson, W. L. Peck, C. B. Grahames, M. A. Casula, Y. Yiangou, R. Birch, P. Anand, G. N. Buell, Disruption of the $P2X_7$ purinoceptor gene abolishes chronic inflammatory and neuropathic pain. *Pain* **114**, 386–396 (2005). Medline doi:10.1016/j.pain.2005.01.002

28. A. M. Basso, N. A. Bratcher, R. R. Harris, M. F. Jarvis, M. W. Decker, L. E. Rueter, Behavioral profile of $P2X_7$ receptor knockout mice in animal models of depression and anxiety: Relevance for neuropsychiatric disorders. *Behav. Brain Res.* **198**, 83–90 (2009). Medline doi:10.1016/j.bbr.2008.10.018

29. B. S. Khakh, M. V. Sofroniew, Diversity of astrocyte functions and phenotypes in neural circuits. *Nat. Neurosci.* **18**, 942–952 (2015). Medline doi:10.1038/nn.4043

30. A. Aguzzi, B. A. Barres, M. L. Bennett, Microglia: Scapegoat, saboteur, or something else? *Science* **339**, 156–161 (2013). Medline doi:10.1126/science.1227901

31. B. Heinke, E. Gingl, J. Sandkühler, Multiple targets of μ-opioid receptor-mediated presynaptic inhibition at primary afferent Aδ- and C-fibers. *J. Neurosci.* **31**, 1313–1322 (2011). Medline doi:10.1523/JNEUROSCI.4060-10.2011

32. H. Dodt, M. Eder, A. Frick, W. Zieglgänsberger, Precisely localized LTD in the neocortex revealed by infrared-guided laser stimulation. *Science* **286**, 110–113 (1999). Medline doi:10.1126/science.286.5437.110

33. R. Ruscheweyh, L. Forsthuber, D. Schoffnegger, J. Sandkühler, Modification of classical neurochemical markers in identified primary afferent neurons with Aβ-, Aδ-, and C-fibers after chronic constriction injury in mice. *J. Comp. Neurol.* **502**, 325–336 (2007). Medline doi:10.1002/cne.21311

34. S. D. Honsek, C. Walz, K. W. Kafitz, C. R. Rose, Astrocyte calcium signals at Schaffer collateral to CA1 pyramidal cell synapses correlate with the number of activated synapses but not with synaptic strength. *Hippocampus* **22**, 29–42 (2012). Medline doi:10.1002/hipo.20843

35. R. Drdla-Schutting, J. Benrath, G. Wunderbaldinger, J. Sandkühler, Erasure of a spinal memory trace of pain by a brief, high-dose opioid administration. *Science* **335**, 235–238 (2012). Medline doi:10.1126/science.1211726